Cancer Letters 449 (2019) 8–19

Contents lists available at ScienceDirect

Cancer Letters

journal homepage: www.elsevier.com/locate/canlet

Original Articles

Src-mediated phosphorylation, ubiquitination and degradation of Caveolin-1 promotes breast cancer cell stemness

Hyo-Jin Yoon[a], Do-Hee Kim[a,b], Su-Jung Kim[a], Jeong-Hoon Jang[a], Young-Joon Surh[a,b,c,*]

[a] Tumor Microenvironment Global Core Research Center, College of Pharmacy, Seoul National University, Seoul, 08826, South Korea
[b] Department of Molecular Medicine and Biopharmaceutical Sciences, College of Pharmacy, Seoul National University, Seoul, 08826, South Korea
[c] Cancer Research Institute, Seoul National University, Seoul, 03080, South Korea

ARTICLE INFO

Keywords:
Breast cancer stem cell
Caveolin-1
c-Src
Phosphorylation
Destabilization

ABSTRACT

Cancer stem cells (CSCs) are responsible for tumor initiation, metastasis and recurrence. Caveolin-1 (Cav-1) is a major protein of caveolae, which participates in various cellular functions, such as vesicle trafficking, cholesterol homeostasis, tumor progression, etc. In the present study, we investigated a role for Cav-1 in regulating the stemness of human breast cancer (MDA-MB-231) cells. Cav-1 expression was significantly lower in tumorspheres than in adherent cells. The silencing of Cav-1 enhanced stemness of MDA-MB-231 cells. Mechanistically, Cav-1 silencing was accompanied by enhanced expression of Bmi-1, which is a representative self-renewal regulator, and promoted epithelial-mesenchymal transition. In a CSC-like state, reduced Cav-1 depends on its destabilization through ubiquitin-proteasome degradation. We further found that Src-mediated phosphorylation of Cav-1 at the Tyr 14 residue is essential for its degradation. Taken together, these findings suggest that Cav-1 destabilization by Src may play a pivotal role in manifestation and maintenance of stemness in breast cancer cells.

1. Introduction

Breast cancer is the most frequently diagnosed cancer and the leading cause of cancer death in women worldwide. In spite of the diverse therapeutic options, chemo-/radioresistance and disease relapse often develop, which is attributed to the presence of stem-like cancer cells in the tumor microenvironment [1,2].

Cancer stem cells (CSCs) are defined as a subset of cancer cells characterized by the property of self-renewal and differentiation, which drive tumorigenesis and tumor heterogeneity [3–5]. Several lines of evidence suggest that epithelial-mesenchymal transition (EMT) and stem cell-like traits are intertwined processes to foster metastatic tumor microenvironment. As an initial step of tumor cell migration, EMT can induce differentiation of cancer cells into a CSC-like state [6]. In this context, CSCs may underlie local and distant metastases by acquiring mesenchymal features which would greatly facilitate systemic dissemination from the primary tumor mass to metastatic tumor [7]. Many of the signaling molecules including Wnt/β-catenin, Notch, Hedgehog, STAT3, and TGF-β are involved in generation and maintenance of CSCs [8–10]. Therefore, therapeutic strategies targeting CSCs by modulating these signaling molecules have attracted special attention.

Caveolin-1 (Cav-1) is a major protein of caveolae, which is flask-shaped invagination at cell membranes. Caveolae participate in various cellular functions, such as vesicle trafficking, cholesterol homeostasis, tumor progression, and especially modulation of various signal transduction pathways [11,12]. Cav-1 is thought to regulate the activity of proteins, such as Src family kinases, H-Ras, protein kinase C, epidermal growth factor tyrosine kinase, extracellular signal-regulated kinase, and endothelial nitric oxide synthase involved in oncogenic signaling pathways [13,14]. Src interaction with the plasma membrane is an important determinant of its activity. For instance, the intrinsic kinase activity of Src phosphorylates Cav-1. Subsequent binding of the activated Src to phosphotyrosylated Cav-1 modulates its association with the membrane [15]. Originally identified as a substrate for v-Src, Cav-1 is phosphorylated on Tyr14 by c-Src [16]. Circumstantial evidence suggests that phosphorylated Cav-1 also regulates its cellular localization and function [17–21]. Collectively, Cav-1 modulates various signaling pathways invloved in breast [22], glioblastoma [23], lung [24], and other cancer types [25].

The role of Cav-1 in development and progression of cancer is controversial because it is suggested to exert both tumor-suppressive and oncogenic effects. In recent studies, Cav-1-mediated signaling has been correlated with maintenance of stemness to augment various cancer stem cells expansion [26]. However, the precise function of Cav-1, particularly in relation to its phosphorylation by Src, in affecting CSCs is largely unknown. Here we report that Src-mediated

* Corresponding author. Tumor Microenvironment Global Core Research Center, College of Pharmacy, Seoul National University, Seoul, 08826, South Korea.
E-mail address: surh@snu.ac.kr (Y.-J. Surh).

https://doi.org/10.1016/j.canlet.2019.01.021
Received 12 November 2018; Received in revised form 2 January 2019; Accepted 14 January 2019

phosphorylation and subsequent destabilization of Cav-1 contributes to maintenance of breast CSCs and manifestation of their characteristics.

2. Materials and methods

2.1. Reagent and antibodies

Dulbecco's modified Eagle's medium (DMEM), Rosewell Park Memorial Institute (RPMI) 1640 medium, Dulbecco's modified Eagle Medium Nutrient Mixture F-12 (DMEM/F-12), and Fetal Bovine Serum (FBS) were purchased from Gibco BRL (Grand Island, NY, USA). TRIzol® was obtained from Invitrogen (Carlsbad, CA, USA). Primary antibodies for Bmi-1, Notch-1, CD133, Sox-2, Src, p-Src, and Ubiquitin were purchased from Cell Signaling Technology (Danvers, MA, USA). Antibodies against Cav-1, Oct 3/4, Snail, and β-actin were obtained from Santa Cruz (Santa Cruz, CA, USA). Antibodies against p-Cav-1, Twist 1, N-cadherin, E-cadherin, CD24 and CD44 were purchased from BD Biosciences (Bedford, MA, USA). The bicinchoninic acid (BCA) protein assay reagent was a product of Pierce Biotechnology (Rockfold, IL, USA). MG-132 was obtained from Enzo Life Sciences (Exeter, UK). The Src inhibitor (PP2) was purchased from EMD Milipore Corporation (Bilierica, MA, USA).

2.2. Cell culture

The human breast cancer cell lines MCF-7, T47D, SKBR3, MDA-MB-453, MDA-MB-231, and MDA-MB-468 were obtained from the American Type Culture Collection (Manassas, VA, USA). MDA-MB-453, MDA-MB-231 and MDA-MB-468 cells were maintained in DMEM, whereas MCF-7, T47D, and SKBR3 cells were maintained in RPMI 1640 cell culture media. All culture media were supplemented with 10% FBS and 1% antibiotics and cultures were grown at 37 °C with 5% CO_2/95% air.

2.3. Tumorsphere culture

For tumorsphere formation from the adherent cells, single cells were cultured in a serum free DMEM/F12 medium supplemented with B27 (GIBCO), 20 ng/mL epidermal growth factor (EGF; Sigma-Aldrich, St. Louis, MO, USA), 20 ng/mL basic fibroblast growth factor (b-FGF; PeproTech, Rocky Hill, NJ, USA) and 4 ng/mL heparin (Sigma-Aldrich). Primary tumorspheres were seeded at a density of 1×10^4 cells/mL in 100 mm ultralow attachment plates (Corning, NY, USA) for 5 consecutive days, and 2 mL of medium was added every 3 days. To culture secondary tumorspheres, primary tumorspheres were gently collected and dissociated into a single-cell suspension using 40 μm strainer. Single cells were counted and then seeded again for another 5 days with addition of 2 mL medium every 3 days. Using the same experimental method, tertiary mammospheres were generated from secondary mammospheres. The number of mammospheres formed (> 100 μm) was counted at indicated times under a microscope. Images were analyzed by using the ImageJ software (http://rsb.info.nih.gov/ij/docs/index.html). 3D picture analysis and quantification were carried out using the ReViSP software (https://sourceforge.net/projects/revisp/).

2.4. Flow cytometry analysis

Cells were collected, washed with phosphate-buffered saline (PBS), and dissociated with Accutase solution (Sigma-Aldrich). Cells were then counted and washed with PBS containing 2% FBS and 0.1% Tween-20. Cells were stained with CD24-PE and CD44-APC for 30 min at 4 °C. After incubation, cells were collected and washed with PBS again. Cells were dissociated into single cells by using 40 μm strainer, and then the population of $CD44^{high}/CD24^{low}$ cells was measured using BD FACSCalibur (Becton Dickinson Biosciences, San Jose, USA).

2.5. ALDEFLUOR assay

The ALDEFLUOR™ kit (StemCell Technologies, Durham, NC, USA) was used to identify the cells that express high levels of the enzyme aldehyde dehydrogenase (ALDH). MDA-MB-231 mammospheres were obtained and suspended in the ALDEFLUOR Assay Buffer containing ALDH substrate at a density of 1×10^5 cells/mL and incubated for 30 min at 37 °C. For negative control, each sample was treated with an ALDH specific inhibitor, diethylaminobenzaldehyde (DEAB), for background fluorescence. The sorting gates were established by eliminating the cells stained positive with ALDH in negative control group. Data were analyzed by the BD FACSCalibur (Becton Dickinson Biosciences).

2.6. Western blot analysis

Whole cell lysate was prepared by scapping the cells in RIPA lysis buffer (150 mM NaCl, 0.5% Triton x 100, 50 mM Tri-HCl (pH 7.4), 25 mM NaF, 20 mM EGTA, 1 mM dithiothreitol, 1 mM Na_3VO_4, 0.1 mM phenylmethane sulfonyl fluoride or phenylmethylsulfonyl fluoride (PMSF), protease inhibitor cocktail tablets) for 15 min on ice followed by centrifugation at 13,000*g* for 15 min. The supernatant containing proteins was collected and stored at −70 °C. For Western blot analysis, the protein concentration of whole cell lysates was measured by using the BCA protein assay kit (Pierce, Rockford, IL, USA). Protein was separated by running through 8–12% SDS-PAGE gel and transferred to the PVDF membrane (Gelman Laboratory, Ann Arbor, MI, USA). The blots were blocked with 5% non-fat dry milk/TBST (Tris-buffered saline buffer containing 0.1% Tween-20) for 1 h at room temperature. The membranes were incubated with the respective primary antibody diluted in TBST overnight 4 °C. Blots were rinsed three times with TBST at 10-min intervals followed by incubation with respective horseradish peroxidase conjugated secondary antibodies (rabbit, mouse or goat) in TBST for 1 h at room temperature. The blots were washed again three times with TBST. The band intensities in Western blotting were visualized with an enhanced chemiluminescent (ECL) detection kit (Amersham Pharmacia Biotech, Buckinghamshire, UK) and quantified with the LAS-4000 Image Analyzer (Fujifilm, Tokyo, Japan).

2.7. Reverse transcription-polymerase chain reaction (RT-PCR)

Total RNA was isolated from each cells by using TRIzol® reagent (Invitrogen, Carlsbad, CA, USA) according to the manufacturer's protocol. To generate the cDNA from RNA, 1 μg of total RNA was reverse transcribed with murine leukemia virus reverse transcriptase (Promega, Madison, WI, USA) for 50 min at 42 °C and again for 15 min at 72 °C. About 1 μL of cDNA was amplified with a PCR mixture (HS Prime Taq 2X Premix, Daejeon, South Korea) in sequential reactions. The primers used for each RT-PCR reactions are as follows: *Cav-1*, 5′-ATG TCT GGG GGC AAA TAC GTA-3′ and 5′–TTG GAA CTT GAA ATT GGC ACC A-3′; *Bmi-1*, 5′-CCA GGG CTT TTC AAA AAT-3′ and 5′-GCA TCA CAG TCA TTG CTG CT-3′; *Notch1*, 5′-GGG TCC ACC AGT TTG AAT GG-3′ and 5′-GTT TGC TGG CTG CAG GTT CT-3′; *Gapdh*, 5′-AAG GTC GGA GTC AAC GGA TTT-3′ and 5′-GCA GTG AGG GTC TCT CTC T-3′; *Twist1*, 5′-GGA GTC CGC AGT CTT ACG AG-3 and 5′-TCT GGA GGA CCT GGT AGA GG-3′; *Snail1,* 5′-CCT GCT GGC AGC CAT CCC AC-3′ and 5′-GGC ACG GTG TGG CTT CGG AT-3′; *Slug,* 5′-ACG CCC AGC TAC CCA ATG GC-3′ and 5′–AGG GCG CCC AGG CTC ACA TA-3′; *Zeb1*, 5′-AGT GAT CCA GCC AAA TGG AA-3′ and 5′-TTT TTG GGC GGT GTA GAA TC-3′ (forward and reverse, respectively). Amplification products were analyzed by 1.5–2% agarose gel electrophoresis, followed by staining with SYBR Green (Invitrogen, Carlsbad, CA, USA) and photographed using fluorescence in LAS-4000 (Fujifilm, Tokyo, Japan).

2.8. Transient transfection of siRNA

MDA-MB-231 cells were seeded at a density of 1×10^5 cell/mL in

100 mm dish in complete growth media. Cav-1 siRNA (25 nM) was transfected into MDA-MB-231 cells with lipofectamine RNAiMAX (Invitrogen) reagent according to the manufacturer's instructions. The target sequence for human Cav-1 siRNA was 5' -AGA CGA GCU GAG CGA GAA GCA UU3' (forward) and 5' -UGC UUC UCG CUC AGC UCG UCU UU-3' (reverse). siRNA oligonucleotide targeting for Cav-1 was purchased from Genolution Pharmaceuticals (Seoul, South Korea).

2.9. Transient transfection of plasmid

Transient transfection of plasmid encoding native or mutant Cav-1 in which tyrosine 14 is replaced by phenylalanine (Y14F-Cav-1) was performed by Lipofectamine® 2000 reagent (Invitrogen, Carlsbad, CA, USA) according to the manufacturer's instructions. After 36-h transfection, cells were harvested or cultured to generate according to purpose of the experiment.

2.10. Immunofluorescent analysis

Human paraffin-embedded breast cancer tissue array (US Biomax, Inc., cat. no. BR1201a; Rockville, MD, USA) was subjected to deparaffinization with xylene. Following antigen retrieval by heated citrate buffer, sections were permeabilized and blocked according to the standard protocol. After overnight incubation at 4 °C with anti-Cav-1, the tissue sections were washed with PBS and then labeled with TRITC-conjugated anti-mouse IgG secondary antibody for 1 h at room temperature. The slides were then analyzed under a fluorescent microscope.

2.11. Immunocytochemical analysis

MDA-MB-231 cells were plated on the 8-well chamber slide (0.5 × cells/well) and transfected with control or Cav-1 specific siRNA. Cells were fixed in 95% methanol for 10 min at −20 °C. After rinse with PBS containing 0.1% Tween 20 (PBST), cells were incubated in 0.2% Triton X-100 in PBS for 5 min. After three washing steps with PBST, cells were blocked for 2 h in fresh blocking buffer [PBST, pH 7.4, containing 5% bovine serum albumin (BSA)]. Dilution (1:100) of primary antibody was made in PBST with 1% BSA, and cells were incubated overnight at 4 °C. After three washing steps with PBST, the cells were incubated with a diluted (1:1000) TRITC-conjugated anti-mouse or FITC-conjugated anti-rabbit IgG secondary antibody in PBST with 1% BSA at room temperature for 1 h. Cells were also stained with 4′,6-diamidino-2-phenylindole (DAPI) and rinsed with PBST. Stained cells were analyzed under a confocal microscope (Leica Microsystems, Heidelberg, Germany) and photographed. The accumulation effects area was quantified using the Image J software.

2.12. Immunoprecipitation

Cells were lysed in 250 mM sucrose, 50 mM Tris-HCl (pH 8.0), 25 mM KCl, 5 mM $MgCl_2$, 1 mM EDTA, 2 μM NaF, 2 μM sodium orthovanadate, 1 mM PMSF and 10 mM N-ethylmaleimide. Total protein (500 μg) was subjected to immunoprecipitation by shaking with Cav-1 primary antibody at 4 °C for 24 h followed by the addition of 20 μL of 25% protein G-agarose bead slurry (Santa Cruz Biotechnology, Inc.; Santa Cruz, CA, USA) and additional shaking for 2 h at 4 °C. After centrifugation at 10,000 *g* for 1 min, immunoprecipitated beads were collected by discarding the supernatant and washed with cell lysis buffer. After final wash, immunoprecipitate was resuspended in 50 μL of 2X SDS electrophoresis sample buffer and boiled for 5 min. 45 μL of supernatant from each sample was loaded on SDS-PAGE. The expression of phosphorylated or ubiquitinated Cav-1 and phosphorylated Src was visualized by antibody against p-Src, p-Cav-1 or ubiquitin.

2.13. Site-directed mutagenesis

Point mutation of tyrosine to phenylalanine at the residue 14 (Y14F) in Cav-1 was induced by using a QuikChange® site-directed mutagenesis kit (Stratagene; Cedar Creek, TX, USA) according to the manufacturer's protocol. Mutant strand synthesis reaction was performed by denaturation at 96 °C for 45 s, annealing at 60 °C for 45 s and extension at 72 °C for 8 min with 30 cycles using the 5.4 kb plasmid template encoding Myc-Cav1. Generally, extension time of 1 min/kb is recommended depending on the length of plasmid template and extension time of 8 min was set as an optimal condition. The following complementary primer pairs were used: sense, 5′-GAC TCG GAG GGA CAT CTC TTC ACC GTT CCC ATC CGG G-3′; antisense, 5′-CCC GGA TGG GAA CGG TGA AGA GAT GTC CCT CCG AGT C-3′. The DNA sequences of all plasmids were verified by sequencing (Cosmo Genetech, Seoul, South Korea).

2.14. Tumorigenesis assay

All animal experiment were approved by the Institutional Animal Care and Use Committee (IACUC) of Seoul National University (authorization number: SNU-160912-1). Six-week-old female BALB/c nude mice (total 12) were purchased from Central Lab Animal, Inc. (Seoul, South Korea) and were maintained under specific pathogen-free (SPF) conditions with 12-h light/12-h dark cycle. After one week of acclimation period, 1×10^4 mock, native (WT-Cav-1) or mutant (Y14F-Cav-1) transfected MDA-MB-231 tumorspheres re-suspended in equal volumes of PBS and matrigel (total volume of 100 μL) were injected into the fourth mammary fat pads of mice. Four mice were included in each group. The tumor incidence was identified by palpation every 3 days. Tumor volume was regularly measured with digital calipers and calculated according to the formula; $V = 0.5\,ab^2$, where 'a' is the longest and 'b' is the shortest perpendicular diameters. After mice were killed, xenograft tumors were excised and fixed in formalin for further analysis.

2.15. Statistical analysis

Data were represented as means of ± standard deviation (SD) at least three independent experiments. Statistical significance was determined by Student's *t*-test and a *p*-value of less than 0.05 was considered to be statistically significant.

3. Results

3.1. Cav-1 is down-regulated in tumorspheres derived from highly invasiveness breast cancer cells

We initially investigated the correlation between Cav-1 expression and clinical progress of breast cancer patients. For this purpose, immunofluorescent analysis was performed to detect the expression of Cav-1 in 120 patients tissues with different clinical stages, including stage 1 (n = 6), stage 2 (n = 94), and stage 3 (n = 20). As shown in Fig. 1A, Cav-1 expression was strongly correlated with clinical stages in breast cancer patients. This finding is corroborated by the microarray data retrieved from the Cancer Genome Atlas analyzed through the oncomine web portal (www.oncomine.org) (Fig. 1B). Likewise, higher expression of Cav-1 was found in MDA-MB-231 and MDA-MB-468 cells, highly invasive breast cancer cell lines (Fig. 1C). Next, we examined whether Cav-1 could be involved in modulating the stemness of breast cancer cells. We enriched for stemness characteristics of breast cancer cells (MCF-7, MDA-MB-453, MDA-MB-231 and MDA-MB-468), by culturing them as spheroids (Fig. 1D and Supplementary Fig. 1A). As shown in Fig. 1E, the expression of CD133, Oct 3/4, and Sox2, well-known stemness markers, was increased in MDA-MB-231 and MDA-MB-

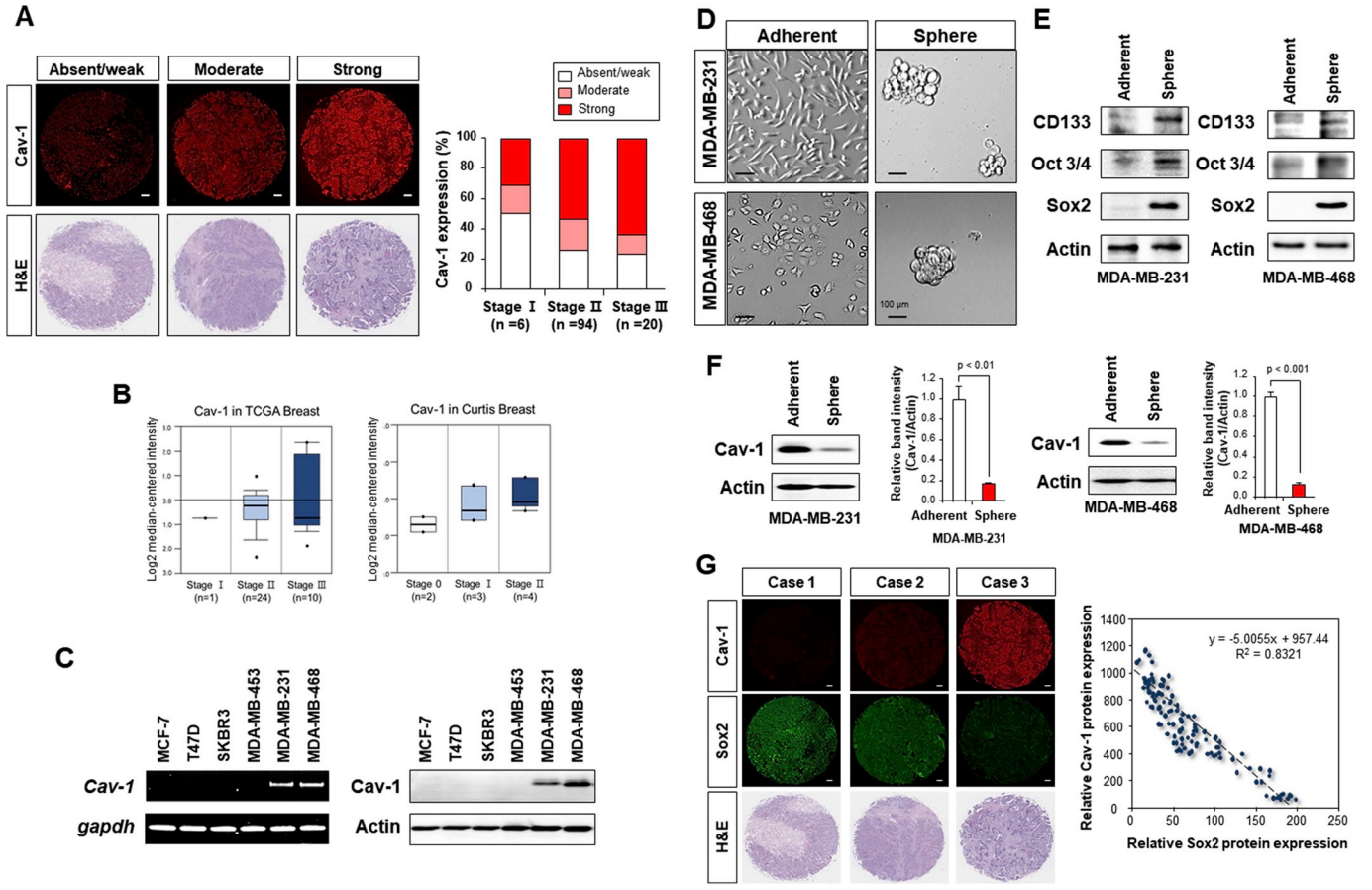

Fig. 1. Repression of Cav-1 expression in the spheroids of basal-like breast cancer cells. (A) Immunofluorescent analysis for Cav-1 expression was classified as absent/weak, moderate, or strong in human breast cancer tissues with different clinical stages. The expression of Cav-1 at different levels in each stages was assessed by immunofluorescence staining, and the relative fluorescence intensity was calculated using Image J, an open platform for Java-based scientific image analysis. Hematoxylin and Eosin (H&E) images were provided by US Biomax Inc. (Rockville, MD, USA). Scale bar = 200 μm. **(B)** The expression level of Cav-1 in human breast cancer tissues grouped by invasive stage was assessed by Oncomine database analysis. **(C)** The mRNA and protein levels of Cav-1 in various subtypes of breast cancer cells were measured by reverse transcription-PCR and Western blot analyses, respectively. **(D)** Tertiary tumorspheres derived from MDA-MB-231 and MDA-MB-468 cells were cultured under sphere-forming conditions. For sphere-forming culture, breast cancer cells were exposed to cancer stem cell medium for 24 h. Cells were cultured in an ultra-low attachment plate to generate primary tumorspheres. After 5 days, primary tumorspheres were counted, collected and replated under the same conditions to form secondary tumorspheres. Using the same experimental method, tertiary mammospheres were generated from secondary mammospheres. The number of mammospheres formed (> 100 μm) was counted under a microscope. Scale bar = 100 μm. **(E)** Expression of stem cell-related marker proteins was analyzed by Western blotting in adherent and sphere cells. **(F)** The expression level of Cav-1 was measured by Western blotting in adherent and sphere cells. The values are expressed as means ± SD (n = 3). **(G)** Immunofluorescent analysis was performed for measuring Cav-1 and Sox2 expression in human breast cancer tissues. The scatter plot demonstrates correlation between Cav-1 and Sox2. Scale bar = 200 μm.

468 tumorspheres. We also observed that tumorspheres derived from MDA-MB-231 and MDA-MB-468 breast cancer cells exhibited much lower levels of Cav-1, compared with adherent cells (Fig. 1F), whereas the protein level of Cav-1 in MCF-7 and MDA-MB-453 cells showed no differences (Supplementary Fig. 1B). Furthermore, immunofluorescent analysis reveals that Cav-1 expression is associated with a stemness marker, Sox2 (Fig. 1G). Based on these observations, Cav-1 is likely to play a crucial role in the stemness of breast cancer cells.

3.2. Silencing of Cav-1 enhances the stemness phenotype of MDA-MB-231 cells

As Cav-1 expression is down-regulated in MDA-MB-231 tumorspheres compared to adherent cells, we carried out an experiment using siRNA to examine the impact of Cav-1 on manifestation of stemness. As shown in Fig. 2A, the silencing of Cav-1 resulted in the elevated expression of the well-known stemness-related proteins, Nanog, Oct 3/4, and Sox2. Consistently, the Cav-1 knockdown increased the size and the number of spheres in MDA-MB-231 (Fig. 2B) and MDA-MB 468 (Supplementary Fig. 2A) cells. Conversely, the tumorsphere-forming capacity in less invasive MCF-7 cells was reduced after overexpression of Cav-1 (Supplementary Fig. 2B). In addition, the proportion of $CD44^{high}$ and $CD24^{low}$ cells was increased when Cav-1 was knocked down in MDA-MB-231 (Fig. 2C) and MDA-MB-468 (Supplementary Fig. 2C) cells. The ALDH activity, which also accounts for major stemness property, was increased by transfection with the Cav-1 siRNA (Fig. 2D). These findings, taken all together, suggest that Cav-1 plays an important role in maintaining a stemness of breast cancer cells.

3.3. Loss of Cav-1 increases the expression of a self-renewal marker, Bmi-1 and EMT markers

As described above, silencing of Cav-1 results in enhancement of stemness in MDA-MB-231 breast cancer cells. Self-renewal is one of the important properties employed by the CSCs to maintain the proliferating capacities. Notch1 and Bmi-1 are known as the key regulators of self-renewal activity in mammary stem cells [27]. In this study, Cav-1 knockdown up-regulated Bmi-1 expression at both mRNA and protein levels, but there was no change in the expression levels of Notch-1 (Fig. 3A and B). Conversely, the Bmi-1 expression was significantly

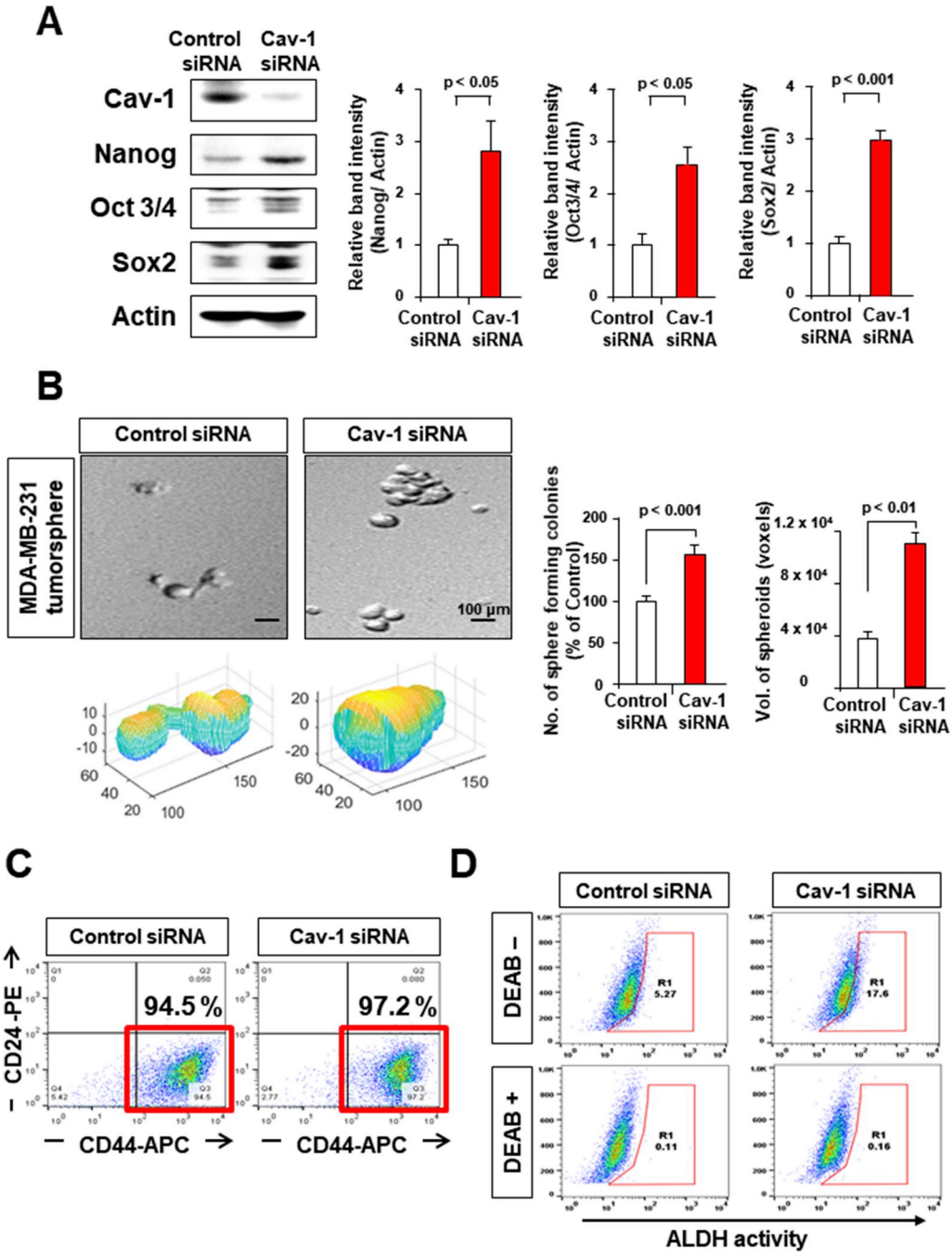

Fig. 2. Enhancement of the stemness of MDA-MB-231 by Cav-1 knockdown. (**A**) The protein levels of Nanog, Oct 3/4 and SOX2 were assessed by Western blot analysis in the MDA-MB-231 cells transfected with control siRNA or specific Cav-1 siRNA for 36 h. The values are expressed as means ± SD (n = 3). **(B)** After control siRNA or Cav-1 siRNA treatment, MDA-MB-231 cells were cultured under sphere-forming condition. Tumorsphere frequencies of Cav-1 knockdown MDA-MB-231 cells were calculated and representative sphere images were visualized under a microscope. The volume of each spheroid was computed by using ReViSP, a software specifically designed to accurately estimate the volume of spheroids and to render an image of their 3D surface. The values are expressed as means ± SD (n = 3). **(C)** Proportions of CD44 ^{high} and CD24^{low} cells were determined by flow cytometry in the MDA-MB 231 cells transfected with control siRNA or specific Cav-1 siRNA for 36 h. The cells were stained with anti-CD44-APC and anti-CD24-PE antibodies. **(D)** Proportions of ALDH^{+} MDA-MB-231 cells were determined by flow cytometry. After cells were treated with control siRNA or specific Cav-1 siRNA for 36 h, the proportions of ALDH^{+} cells were determined by FACS analysis. Lower part: negative control obtained by treating cells with DEAB, an irreversible inhibitor or ALDH activity. Levels of a specific fluorescence were set as background. Upper part: specific ALDH-dependent fluorescence levels in control siRNA or Cav-1 siRNA treated cells. y-axis: side scatter distribution of the tested cell populations. x-axis: distribution of fluorescent cells in the tested cell populations. The values are expressed as means ± SD (n = 3).

decreased after overexpression of Cav-1 in MCF-7 cells (Supplementary Figs. 3A and 3B). Since acquisition of stem-like traits has been linked to EMT properties [28,29], we also investigated the role of Cav-1 in the induction of EMT in MDA-MB-231 cells. The induction of EMT leads to the loss of epithelial characteristics (such as E-cadherin, desmoplakin and claudins) and an acquisition of mesenchymal phenotype (vimentin, α5β1integrin and fibronectin) [30,31]. Cav-1 inhibition increased the expression of EMT marker genes, such as *Snail*, *Twist1*, and *N-Cadherin* (Fig. 3C) and their protein products (Fig. 3D). An immunocytochemistry assay verified the upregulation of N-cadherin and snail in Cav-1 knockdown cells (Fig. 3E). Although loss of E-cadherin is a key feature of EMT, it was difficult to identify the tendency of E-cadherin decrease as the cells used in this study express a relatively low level of this protein (Supplementary Fig. 4). We next determined whether Bmi-1 could affect EMT signaling. siRNA-mediated silencing of Bmi-1 markedly reduced the mRNA and protein expression of EMT markers in MDA-MB-231 cell (Fig. 3F and G). These results suggest that Bmi-1 induced by the Cav-1 downregulation plays a role in stimulating EMT in a MDA-MB-231 breast cancer cells.

3.4. Expression of the Cav-1 protein, but not its mRNA transcript, is reduced as a consequence of proteasomal degradation in MDA-MB-231 tumorspheres

In contrast to no significant difference in Cav-1 mRNA expression levels between the adherent and the tumorsphere cells, MDA-MB-231 derived tumorspheres exhibited marked reduction in the steady state level of the Cav-1 protein (Fig. 4A). To determine whether acquisition of stemness is a consequence of Cav-1 protein destabilization, we monitored the degradation of Cav-1 in tumorsphere as well as adherent

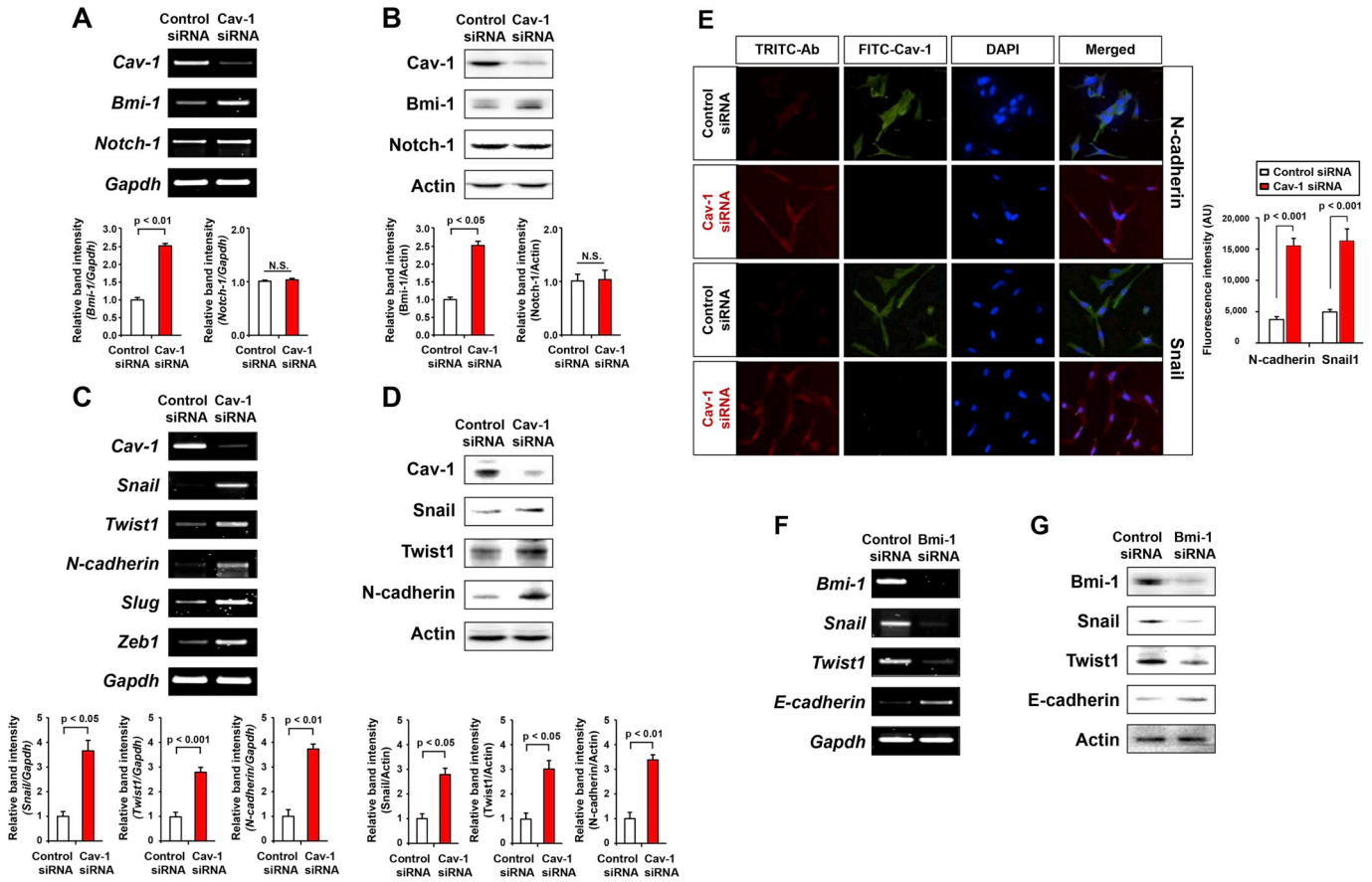

Fig. 3. Up-regulation of Bmi-1 and EMT markers in Cav-1 knockdown MDA-MB-231 cells. MDA-MB-231 cells were transfected with control siRNA or specific Cav-1 siRNA for 36 h. (**A, B**) RT-PCR and Western blot analysis were performed to detect expression of self-renewal marker genes, *Bmi-1* and *Notch-1* and their protein products, respectively. N.S., not significant (**C, D**) The mRNA and protein levels of EMT markers were determined by RT-PCR and Western blot analysis, respectively. **(E)** Immunocytochemical analysis was performed using antibodies against N-cadherin and Snail. Conditions for Cav-1 knockdown MDA-MB-231 cells are same as described in (**A**). Cells stained with DAPI were visualized by fluorescent microscopy. Relative mean fluorescence intensity was calculated using Image J. (**F, G**) RT-PCR and Western blot analysis of EMT markers in MDA-MB-231 cells that were transfected with non-specific or Bmi-1 specific siRNA for 36 h. GAPDH and β-actin were used as a loading control.

cells after inhibition of *de novo* protein synthesis by cycloheximide. As illustrated in Fig. 4B, Cav-1 in the MDA-MB-231 tumorspheres underwent degradation rapidly as compared with adherent cells after addition of cycloheximide. Many labile proteins are commonly degraded via the ubiquitin-proteasomal pathway. As shown in Fig. 4C, treatment of MDA-MB-231 tumorspheres with the proteasome inhibitor, MG-132 resulted in restoration of Cav-1. Generally, proteins subjected to proteasomal degradation are marked by prior attachment of ubiquitin to their lysine residue. As illustrated in Fig. 4D, MDA-MB-231 tumorspheres exhibited enhanced ubiquitiation of Cav-1 with a concomitant acquisition of stem-like properties compared to adherent cells (Fig. 4D).

3.5. Role of Src in phosphorylation and stability of Cav-1 in MDA-MB-231 tumorspheres

Src has a kinase activity which contributes to its association with Cav-1. Thus, binding of Src to phosphotyrosylated Cav-1 affects Cav-1-regulated signaling [12,32]. This prompted us to examine whether Cav-1-Src interaction was involved in the maintenance of stemness in breast cancer cells. As shown in Fig. 5A, the expression of p-Cav-1 (Tyr^{14}) and p-Src (Tyr^{416}) was much higher in tumorsphere cells, compared to adherent cells. In line with the notion that Src-dependent phosphorylation targets Cav-1 for degradation, PP2, a specific Src inhibitor, abrogated Cav-1 phosphorylation in MDA-MB-231 tumorspheres (Fig. 5B). These findings suggest that sustained phosphorylation of Cav-1 (Tyr^{14}) by active Src accounts for Cav-1 degradation. Moreover, PP2 treatment attenuated Cav-1 ubiquitination (Fig. 5C), the characteristic signature of proteasomal targeting. Consistently, the Cav-1 expression repressed in MDA-MB-231 tumorspheres was restored after addition of PP2, whereas the expression levels of Cav-1 in the adherent cells had no differences (Fig. 5D). In addition, treatment of MDA-MB-231 tumorspheres with PP2 decreased the size and the number of spheres (Fig. 5E). Thus, it is likely that destabilization of Cav-1 in tumorsphere occurs by Src-dependent phosphorylation of Cav-1 (Tyr^{14}).

3.6. Tyrosine 14 of Cav-1 is a key amino acid in maintaining stemness of breast cancer

The tyrosine 14 residue of Cav-1 is thought to be the principal site for recognition by c-Src kinase. To ensure this tyrosine residue is implicated in the regulation of Cav-1, we mutated the tyrosine 14 to phenylalanine, which eliminated the phosphorylation site. The mutant construct (Y14F Cav-1) was then transfected into MDA-MB-231 cells. Analysis of each of the transfected lines revealed that the Y14F Cav-1 mutation was sufficient to abolish phosphorylation and ubiquitination of Cav-1 expression (Fig. 6A and B). To verify that Cav-1 suppresses the breast cancer cell stemness, we overexpressed Cav-1 in MDA-MB-231 tumorspheres. As a result, the MDA-MB-231 tumorspheres overexpressing WT-Cav-1 reduced the ability of spheroid formation compared with MOCK cells. Additionally, the tumorsphere-forming ability of cells expressing Y14F mutant Cav-1 was weaker than that of cells expressing WT-Cav-1 (Fig. 6C). Consistent with this finding, the Y14F

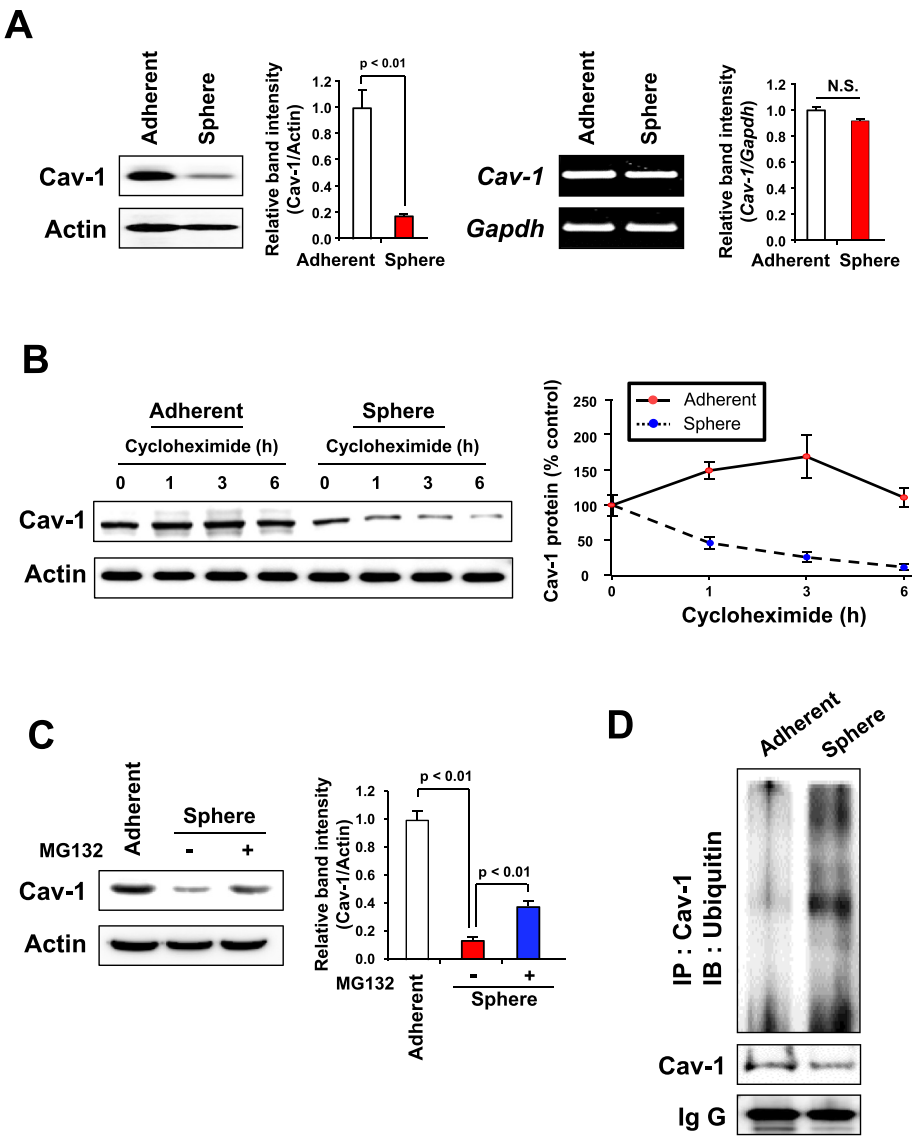

Fig. 4. Enhanced ubiquitination and proteasomal degradation of Cav-1 protein in MDA-MB-231 tumorspheres. **(A)** MDA-MB-231 cells were cultured on ultra-low attachment plates for 5 days to generate primary tumorspheres, and then were dissociated into single cell suspension to generate secondary tumorspheres for 5 days. Using the same experimental method, tertiary tumorspheres were generated from secondary tumorspheres. The expression of Cav-1 and its mRNA transcript was determined by Western blot and RT-PCR analyses, respectively in adherent and MDA-MB-231 tumorspheres. β-Actin and *gapdh* were used as a loading or internal control. N.S., not significant **(B)** To monitor the protein stability, adherent and MDA-MB-231 tumorspheres were treated with 70.07 μM of cycloheximide (CHX), and the expression levels of Cav-1 was measured at indicated time points. **(C)** Tertiary tumorsphere cells were treated with or without 20 μM of MG-132, and expression levels of Cav-1 were determined by Western blot analysis as compared to adherent cells. The values are presented means ± SD (n = 3). **(D)** To assess the ubiquitination of Cav-1, adherent and MDA-MB-231 tumorspheres were immunoprecipitated with anti-Cav-1 antibody, followed by Western blot analysis with anti-ubiquitin antibody.

Cav-1 mutation significantly mitigated the retarding effects of Cav-1 on the expression of Bmi-1 and EMT markers (Fig. 6D and E). Similar results were observed in MDA-MB-468 cells (Supplementary Fig. 5). Thus, tyrosine 14 is considered a key amino acid within Cav-1 that regulates stemness capacity in breast cancer cells.

3.7. Tyrosine 14 of Cav-1 is essential for the tumorigenicity of MDA-MB-231 tumorspheres

After finding that phosphorylation of tyrosine 14 of Cav-1 is pivotal to the stem-like properties of breast cancer cells *in vitro*, we assessed whether this amino acid residue would affect the oncogenicity of MDA-MB-231 tumorspheres. The tumorigenic ability was measured for MDA-MB-231 tumorspheres, which were transfected with mock, WT-Cav-1 or Y14F-Cav-1 mutant construct and inoculated into the mammary pads of BALB/c nude mice. The representative image of the excised tumors at the day 40 after inoculation is presented in Fig. 7A. As shown in Fig. 7B, the tumors derived from tumorspheres harbouring Y14F-Cav-1 appeared to have longer latency than those from mock and WT-Cav-1 tumorsphere groups. After 40 days, the volume and the weight formed in the Y14F-Cav-1 tumorsphere group were markedly reduced compared with those in mock and WT-Cav-1 tumorsphere groups (Fig. 7C and D).

Hematoxylin-eosin (H&E) staining showed the presence of prominent apoptotic figures in MOCK tumorsphere groups, in contrast to tumors isolated from tumorsphere groups and Y14F-Cav-1 tumorsphere groups containing less apoptotic cells. Immunohistochemical analysis also showed a relatively weaker nuclear staining of pCav-1 in the tumor tissues of mice transplanted with Y14F-Cav-1 spheres (Fig. 7E).

4. Discussion

Chemo-resistance and disease relapse in cancer are attributed to a small subset of cancer stem cells (CSCs) with the capability of self-renewal and differentiation [33,34]. Cancer cells, after invading into the extracellular matrix, enter the microvasculature of the lymph and blood, survive and translocate through the bloodstream. Circulating tumor cells exit from the bloodstream, colonize distant organs and become disseminated tumor cells. Several studies have demonstrated association between stemness and the metastatic potential of disseminated tumor cells [28,35–37]. In the tumor progression, disseminated cancer cells may display a more mesenchymal phenotype, bestowing these cells with stem-like traits. The transformed cells with stem-like traits can migrate from the primary tumor to the bone marrow, due to their capacity to perform the EMT. CSCs localize in the pre-metastatic niche, a distinct region responsible for metastatic

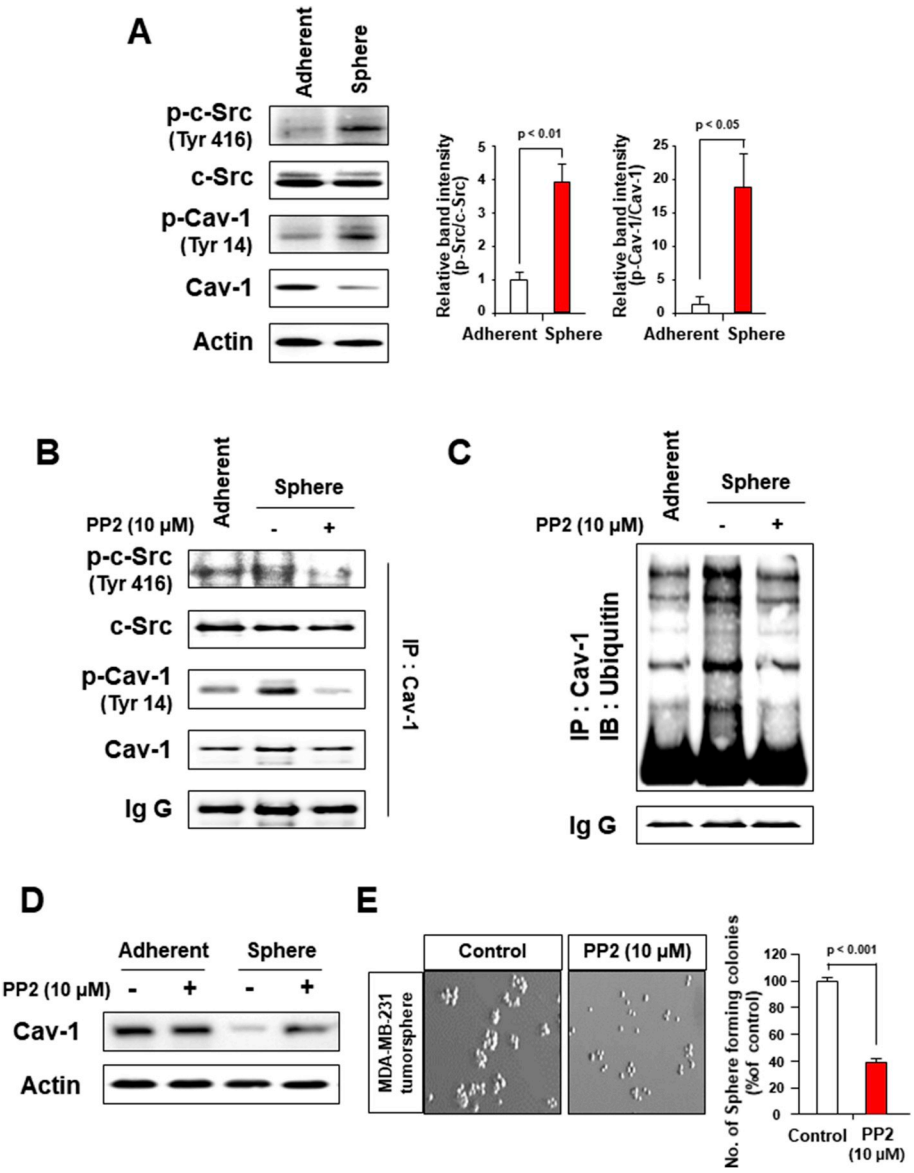

Fig. 5. Effect of Src on phosphorylation and stability of Cav-1 in MDA-MB-231 tumorspheres. (A) The expression levels of total and Tyr416 phosphorylated Src and Cav-1 phosphorylated at Tyr14 were measured by Western blot analysis in adherent and MDA-MB-231 tumorspheres. The values are presented means ± SD (n = 3). **(B)** Tertiary tumorspheres were treated with PP2 (10 μM) or DMSO for 24 h before the sample collection. Src and Cav-1 phosphorylated at Tyr416 and Tyr14, respectively as well as their total forms in adherent and MDA-MB-231 tumorspheres were measured by immunoprecipitation with anti-Cav-1 antibody, followed by immunoblot analysis with antibodies against corresponding antibodies. **(C)** The ubiquitination of Cav-1 was measured by immunoprecipitation as described in the legend to Fig. 4D. **(D)** Following treatment of adherent and tertiary tumorsphere cells with PP2 (10 μM) or DMSO, the protein level of Cav-1 was examined by Western blot analysis. **(E)** The effects of PP2 on tumorsphere formation was confirmed by the tumorsphere assay. Alterations in the shape of tumorspheres were examined by phase-contrast microscopy. The histogram represents the number of spheres that were bigger than 100 μm. The values are indicated as means ± S.D. (n = 3).

progression [38–41]. According to the model of CSCs, a small subpopulation of cancer cells is endowed with stem like traits with the potential to promote cancer progression [42]. CSCs are also primarily responsible for the recurrence of cancer. Therefore, eradication of CSCs in tumors may represent an effective anticancer therapeutic strategy. So far, substantial efforts have been made to explore the signaling pathways modulating self-renewal and differentiation of CSCs, in an attempt to develop regimens or therapeutic strategies targeting CSCs [43,44].

Several lines of evidence suggest that Cav-1 may function as a regulator of self-renewal signaling pathways in stem cells [45,46]. In various cancer types, Cav-1 levels vary during the course of tumor progression. It has been speculated that Cav-1 acts both as a tumor suppressor and an oncogene, depending on the stage of neoplastic transformation and extent of tumor progression [47,48]. Cav-1 is downregulated in early stages facilitating oncogenic transformation, while restoration of Cav-1 in later stages possibly contributes to the development of invasiveness and drug resistance [47]. However, the precise function of Cav-1 on acquisition of stem cell-like properties in cancer progression is largely unknown.

The tumorsphere culture system has been widely used to identify and enrich for putative CSCs from cancer cell lines or primary tumors [49]. In this study, four human breast cancer cell lines representing the major molecular subtypes of breast cancer (Luminal; MCF-7, HER2; MDA-MB-453, Basal-like; MDA-MB-231 and MDA-MB-468) were exploited to generate tumorspheres. We observed that tumorspheres derived from breast cancer cells exhibited much lower levels of Cav-1, compared with adherent cells. Silencing of Cav-1 with siRNA induced stemness properties as evidenced by increased $CD44^{high}/CD24^{low}$ cell population, ALDH activity, expression of stemness-related genes and tumorsphere formation. Recently, the $CD44^{high}/CD24^{low}$ and $ALDH^{+}$ phenotypes are less frequently utilized to identify of CSCs, because their expression is not consistent even in the same molecular subtype of breast cancer. Systematic comparison of their functions is also still insufficient [50,51]. Nevertheless, their expression is still used to identify breast CSCs. Another frequently used stem cell marker is Oct4 (octamer-binding transcription factor 4). According to a hierarchy of breast cancer cells proposed by Patel et al. [52], there is a subset of cells with the least maturity that express a high level of Oct4. This most immature subset of $Oct4^{high}$ breast cancer cells exhibits chemoresistance, dormancy, and stem cell properties, such as self-renewal, serial passaging ability, cycling quiescence, long doubling time, asymmetric division, high metastatic and invasive capability.

Several studies highlighted the role of cadherins and integrins, not only in the regulation of EMT but also in maintaining CSC [53–55].

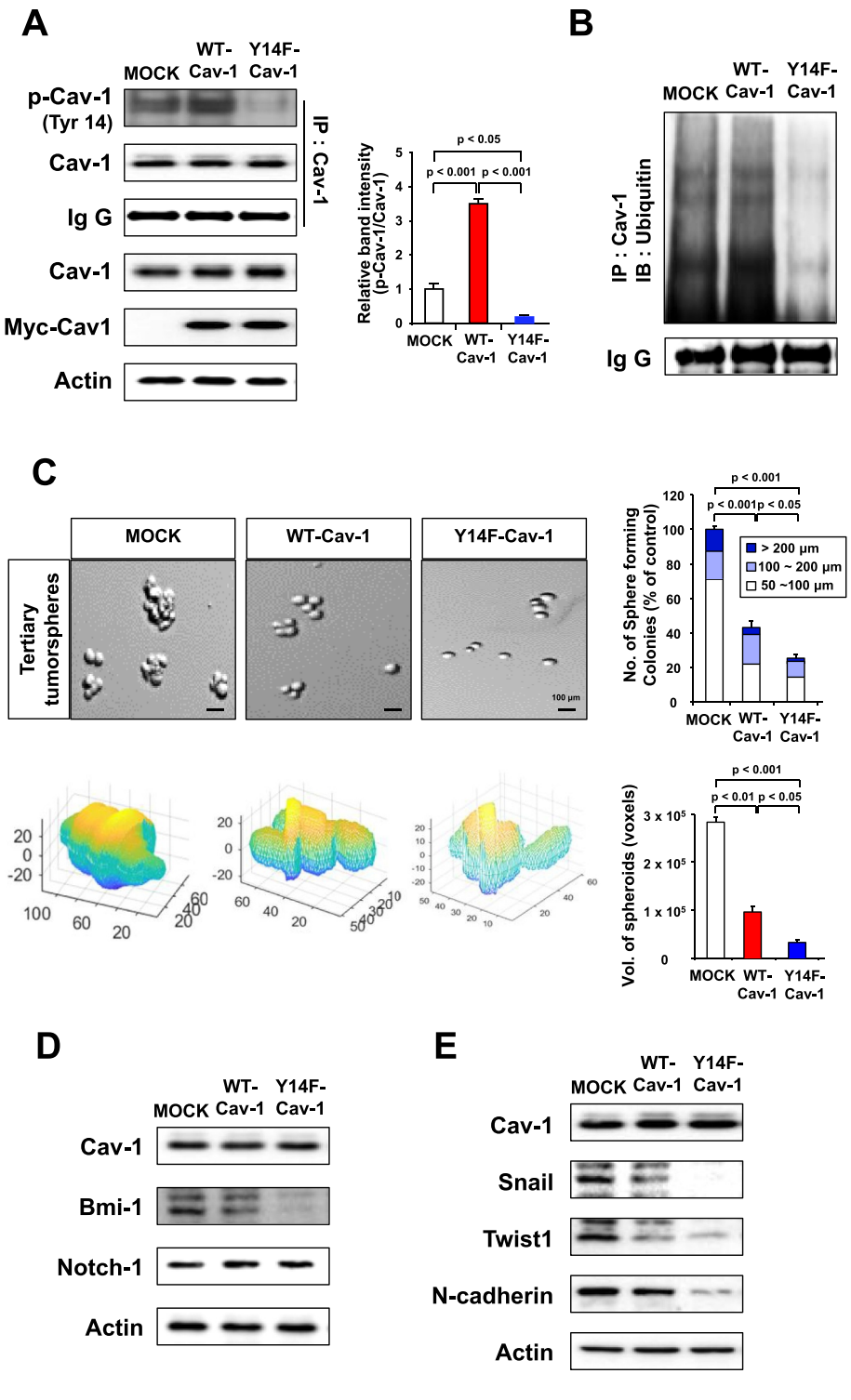

Fig. 6. Essential role of tyrosine 14 of Cav-1 in maintaining stemness of breast cancer cells *in vitro*. MDA-MB-231 cells were transiently transfected with Myc-tagged wild-type (WT-Cav-1) or mutant-Cav1 (Y14F-Cav-1). **(A)** The tyrosine phosphorylation of Cav-1 was detected by immunoprecipitation followed by immunoblot analysis. The expression levels of Cav-1 and myc-tagged Cav-1 in clones expressing MOCK (vector alone) or WT-Cav-1/Y14F-Cav-1 (vector containing myc-tagged Cav-1) were measured by Western blot analysis. **(B)** The ubiquitination of Cav-1 was measured by immunoprecipitation. **(C)** Tumorsphere-forming ability was calculated, and representative sphere images were visualized under a microscope. The volume of each spheroid was computed by using ReViSP, a software specifically designed to accurately estimate the volume of spheroids and to render an image of their 3D surface. The values are expressed as means ± SD (n = 3). The expression level of self-renewal **(D)** and EMT markers **(E)** were analyzed by Western blotting.

Consistent with these findings, we noticed that the expression of α5β1 integrin was increased in tumorspheres (Supplementary Fig. 6). Furthermore, Cav-1 expression has been found to be significantly associated with α5β1 integrin [56]. Results from our present study suggest that Cav-1 knockdown led to EMT which endows breast cancer cells with stem-like features. Similar effects of Cav-1 on stemness were also observed in other cancer cell lines [57], further confirming that Cav-1 plays a role in the cancer progression.

Decreased protein expression of Cav-1 in tumorspheres is not attributable to reduced expression of its mRNA transcript, but rather due to lowered protein stability. It has been reported that phosphorylation of Cav-1 at tyrosine 14 reduces Cav-1 protein stability by facilitating the ubiquitination and proteasomal degradation [58]. Cav-1 is mainly phosphorylated on tyrosine 14 by Src kinase [15,19,59]. Phosphorylation on Tyr 14 by Src is clearly relevant to Cav-1 functions in a number of settings, such as EGF-induced caveolae formation [60], integrin-regulated membrane microdomain internalization [61], and association with the membrane type-I matrix metalloproteinase [19]. Our finding reveals that the tyrosine residue at position 14 of Cav-1 is required for its modulating spheroid formation, and acquiring EMT and stem-like traits. Cav-1 mutation by replacing the Tyr14 with phenylalanine significantly impaired tumorigenic ability of tumorspheres derived from human breast cancer cells.

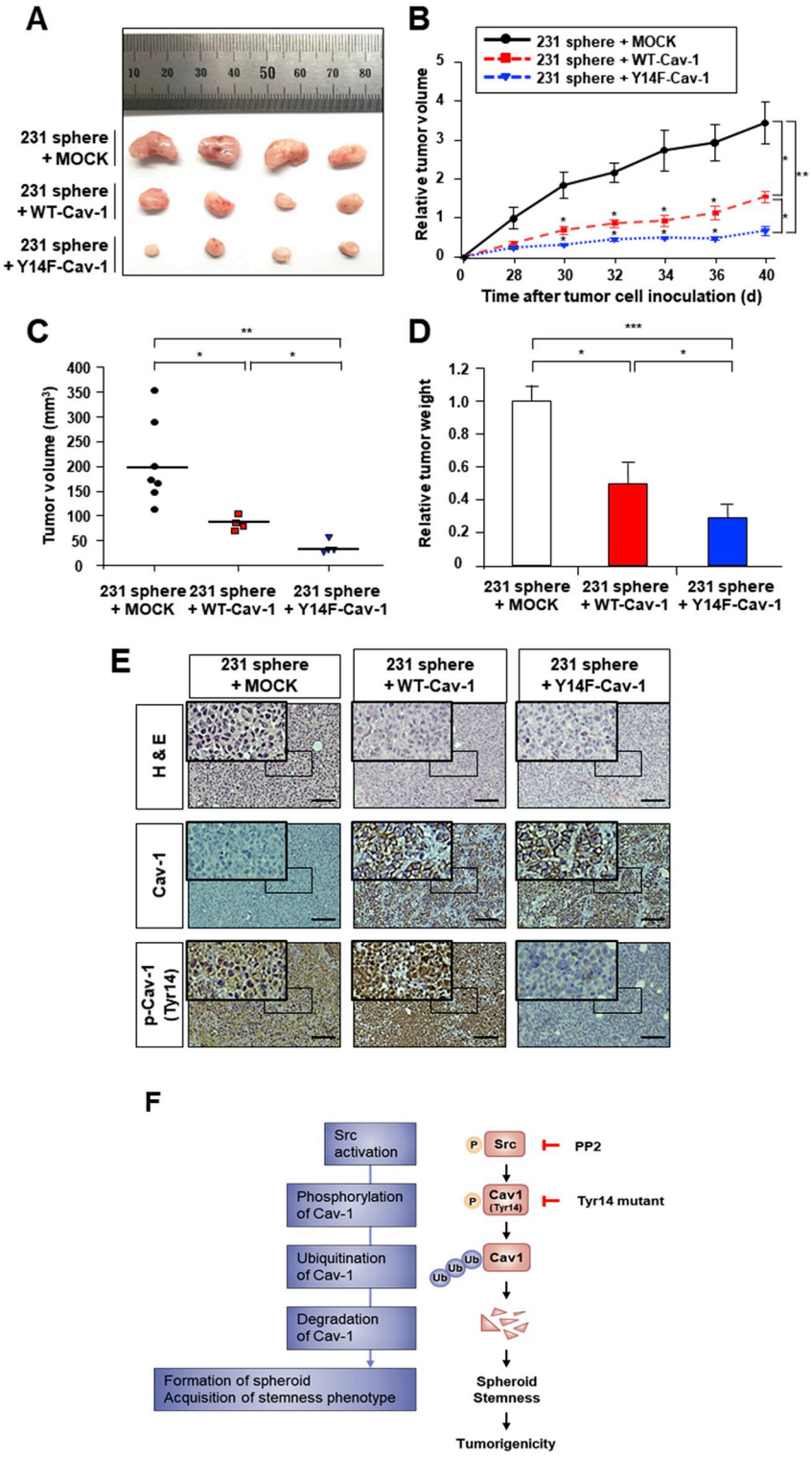

Fig. 7. A critical role of tyrosine 14 of Cav-1 in growth and proliferation of MDA-MB-231 tumorspheres transplanted to nude mice. MDA-MB-231 cells transfected with mock or Myc-tagged wild-type (WT-Cav-1) or mutant-Cav1 (Y14F-Cav-1) were cultured in cultured in ultra-low attachment plates and then passaged to tertiary tumorspheres as described in Materials and methods. A total 1×10^4 cells were injected into the mammary fat pad of BALB/c nude mice. **(A)** Representative tumor images excised from mice at the end of the experiment at the day 40. **(B)** The tumor volume was measured by using the following formula; Volume (V) = 0.5 × longest diameter × (shortest diameter)^2. The values are indicated as means ± S.D. of six xenografts for each group, $^*p < 0.05$, $^{**}p < 0.01$. **(C)** Histograms of the mean tumor volume of each group. Mean tumor volume for each group was calculated at 40 days after injection. **(D)** The tumor weight was measured at the end of the experiment. The results are expressed as means ± SD., $^*p < 0.05$, $^{**}p < 0.01$, $^{***}p < 0.001$. **(E)** Immunohistochemical stains of Cav-1 and p-Cav-1 in tumors from mice. Scale bar = 200 μm. **(F)** Schematic diagram for Src-mediated phosphorylation, ubiquitination, and degradation of Cav-1, facilitating the spheroid formation and acquisition of stemness in breast cancer cells.

In summary, the down-regulation of Cav-1 is detected in breast CSC-like cells, which is associated with upregulation of Bmi-1 and EMT markers. Cav-1 negatively regulates CSC markers, including CD133, Oct 3/4, and Sox2 and tumor spheroid formation, a key feature of CSCs. Down-regulation of Cav-1 is attributed to its destabilization through the Src-mediated phosphorylation at the Tyr14 and subsequent degradation via the ubiquitin-proteasome pathway. Cav-1 destabilized cells exhibit stem-like characteristics which facilitate the formation of tumorspheres and enhance the tumorigenicity (Fig. 7F). Together, our results unveil a novel mechanism of CSC regulation, which could be crucial in understanding the aggressive behaviors of cancer cells and in identifying potential targets for CSC therapy.

Conflicts of interest

The authors declare no conflict of interest.

Acknowledgements

This study was supported by the Global Core Research Center

(GCRC) grant (No. 2011-0030001) from the National Research Foundation (NRF) of Republic of Korea.

Appendix A. Supplementary data

Supplementary data to this article can be found online at https://doi.org/10.1016/j.canlet.2019.01.021.

References

[1] C.A. Pinto, E. Widodo, M. Waltham, E.W. Thompson, Breast cancer stem cells and epithelial mesenchymal plasticity - implications for chemoresistance, Cancer Lett. 341 (2013) 56–62.

[2] F. Al-Ejeh, C.E. Smart, B.J. Morrison, G. Chenevix-Trench, J.A. Lopez, S.R. Lakhani, M.P. Brown, K.K. Khanna, Breast cancer stem cells: treatment resistance and therapeutic opportunities, Carcinogenesis 32 (2011) 650–658.

[3] R. Pardal, M.F. Clarke, S.J. Morrison, Applying the principles of stem-cell biology to cancer, Nat. Rev. Canc. 3 (2003) 895–902.

[4] N.P. Nguyen, F.S. Almeida, A. Chi, L.M. Nguyen, D. Cohen, U. Karlsson, V. Vinh-Hung, Molecular biology of breast cancer stem cells: potential clinical applications, Cancer Treat Rev. 36 (2010) 485–491.

[5] C. Ginestier, E. Charafe-Jauffret, D. Birnbaum, Targeting breast cancer stem cells: fishing season open!, Breast Cancer Res. 12 (2010) 312.

[6] G. van der Horst, L. Bos, G. van der Pluijm, Epithelial plasticity, cancer stem cells, and the tumor-supportive stroma in bladder carcinoma, Mol. Canc. Res. 10 (2012) 995–1009.

[7] I. Malanchi, Tumour cells coerce host tissue to cancer spread, BoneKEy Rep. 2 (2013) 371.

[8] S.D. Fouse, J.F. Costello, Cancer stem cells activate STAT3 the EZ way, Cancer Cell 23 (2013) 711–713.

[9] C. Karamboulas, L. Ailles, Developmental signaling pathways in cancer stem cells of solid tumors, Biochim. Biophys. Acta 1830 (2013) 2481–2495.

[10] E.L. Abhold, A. Kiang, E. Rahimy, S.Z. Kuo, J. Wang-Rodriguez, J.P. Lopez, K.J. Blair, M.A. Yu, M. Haas, K.T. Brumund, X. Altuna, A. Patel, R.A. Weisman, W.M. Ongkeko, EGFR kinase promotes acquisition of stem cell-like properties: a potential therapeutic target in head and neck squamous cell carcinoma stem cells, PLoS One 7 (2012) e32459.

[11] M. Hino, H. Doihara, K. Kobayashi, M. Aoe, N. Shimizu, Caveolin-1 as tumor suppressor gene in breast cancer, Surg. Today 33 (2003) 486–490.

[12] U.E. Martinez-Outschoorn, F. Sotgia, M.P. Lisanti, Caveolae and signalling in cancer, Nat. Rev. Canc. 15 (2015) 225–237.

[13] T. Okamoto, A. Schlegel, P.E. Scherer, M.P. Lisanti, Caveolins, a family of scaffolding proteins for organizing "preassembled signaling complexes" at the plasma membrane, J. Biol. Chem. 273 (1998) 5419–5422.

[14] S. Li, J. Couet, M.P. Lisanti, Src tyrosine kinases, Galpha subunits, and H-Ras share a common membrane-anchored scaffolding protein, caveolin. Caveolin binding negatively regulates the auto-activation of Src tyrosine kinases, J. Biol. Chem. 271 (1996) 29182–29190.

[15] E. Gottlieb-Abraham, D.E. Shvartsman, J.C. Donaldson, M. Ehrlich, O. Gutman, G.S. Martin, Y.I. Henis, Src-mediated caveolin-1 phosphorylation affects the targeting of active Src to specific membrane sites, Mol. Biol. Cell 24 (2013) 3881–3895.

[16] A.N. Shajahan, A. Wang, M. Decker, R.D. Minshall, M.C. Liu, R. Clarke, Caveolin-1 tyrosine phosphorylation enhances paclitaxel-mediated cytotoxicity, J. Biol. Chem. 282 (2007) 5934–5943.

[17] H. Lee, D. Volonte, F. Galbiati, P. Iyengar, D.M. Lublin, D.B. Bregman, M.T. Wilson, R. Campos-Gonzalez, B. Bouzahzah, R.G. Pestell, P.E. Scherer, M.P. Lisanti, Constitutive and growth factor-regulated phosphorylation of caveolin-1 occurs at the same site (Tyr-14) in vivo: identification of a c-Src/Cav-1/Grb7 signaling cassette, Mol. Endocrinol. 14 (2000) 1750–1775.

[18] A.N. Shajahan, C. Tiruppathi, A.V. Smrcka, A.B. Malik, R.D. Minshall, Gbetagamma activation of Src induces caveolae-mediated endocytosis in endothelial cells, J. Biol. Chem. 279 (2004) 48055–48062.

[19] L. Labrecque, C. Nyalendo, S. Langlois, Y. Durocher, C. Roghi, G. Murphy, D. Gingras, R. Beliveau, Src-mediated tyrosine phosphorylation of caveolin-1 induces its association with membrane type 1 matrix metalloproteinase, J. Biol. Chem. 279 (2004) 52132–52140.

[20] A.L. Kiss, A. Turi, N. Mullner, E. Kovacs, E. Botos, A. Greger, Oestrogen-mediated tyrosine phosphorylation of caveolin-1 and its effect on the oestrogen receptor localisation: an in vivo study, Mol. Cell. Endocrinol. 245 (2005) 128–137.

[21] Y.G. Ko, P. Liu, R.K. Pathak, L.C. Craig, R.G. Anderson, Early effects of pp60(v-src) kinase activation on caveolae, J. Cell. Biochem. 71 (1998) 524–535.

[22] S.L. Anwar, A. Wahyono, T. Aryandono, S.J. Haryono, Caveolin-1 in breast cancer: single molecule regulation of multiple key signaling pathways, Asian Pac. J. Cancer Prev. APJCP 16 (2015) 6803–6812.

[23] K. Quann, D.M. Gonzales, I. Mercier, C. Wang, F. Sotgia, R.G. Pestell, M.P. Lisanti, J.F. Jasmin, Caveolin-1 is a negative regulator of tumor growth in glioblastoma and modulates chemosensitivity to temozolomide, Cell Cycle 12 (2013) 1510–1520.

[24] P.G. Lloyd, Caveolin-1, antiapoptosis signaling, and anchorage-independent cell growth. Focus on "Caveolin-1 regulates Mcl-1 stability and anoikis in lung carcinoma cells", Am. J. Physiol. Cell Physiol. 302 (2012) C1282–C1283.

[25] Z.C. Nwosu, M.P. Ebert, S. Dooley, C. Meyer, Caveolin-1 in the regulation of cell metabolism: a cancer perspective, Mol. Canc. 15 (2016) 71.

[26] S. Luanpitpong, L. Wang, T.A. Stueckle, W. Tse, Y.C. Chen, Y. Rojanasakul, Caveolin-1 regulates lung cancer stem-like cell induction and p53 inactivation in carbon nanotube-driven tumorigenesis, Oncotarget 5 (2014) 3541–3554.

[27] A. Borah, S. Raveendran, A. Rochani, T. Maekawa, D.S. Kumar, Targeting self-renewal pathways in cancer stem cells: clinical implications for cancer therapy, Oncogenesis 4 (2015) e177.

[28] S.A. Mani, W. Guo, M.J. Liao, E.N. Eaton, A. Ayyanan, A.Y. Zhou, M. Brooks, F. Reinhard, C.C. Zhang, M. Shipitsin, L.L. Campbell, K. Polyak, C. Brisken, J. Yang, R.A. Weinberg, The epithelial-mesenchymal transition generates cells with properties of stem cells, Cell 133 (2008) 704–715.

[29] M. Santisteban, J.M. Reiman, M.K. Asiedu, M.D. Behrens, A. Nassar, K.R. Kalli, P. Haluska, J.N. Ingle, L.C. Hartmann, M.H. Manjili, D.C. Radisky, S. Ferrone, K.L. Knutson, Immune-induced epithelial to mesenchymal transition in vivo generates breast cancer stem cells, Cancer Res. 69 (2009) 2887–2895.

[30] N. Bednarz-Knoll, C. Alix-Panabieres, K. Pantel, Plasticity of disseminating cancer cells in patients with epithelial malignancies, Cancer Metastasis Rev. 31 (2012) 673–687.

[31] C.S. Scanlon, E.A. Van Tubergen, R.C. Inglehart, N.J. D'Silva, Biomarkers of epithelial-mesenchymal transition in squamous cell carcinoma, J. Dent. Res. 92 (2013) 114–121.

[32] M.P. Lisanti, P.E. Scherer, Z. Tang, M. Sargiacomo, Caveolae, caveolin and caveolin-rich membrane domains: a signalling hypothesis, Trends Cell Biol. 4 (1994) 231–235.

[33] L.V. Nguyen, R. Vanner, P. Dirks, C.J. Eaves, Cancer stem cells: an evolving concept, Nat. Rev. Canc. 12 (2012) 133–143.

[34] K. Chen, Y.H. Huang, J.L. Chen, Understanding and targeting cancer stem cells: therapeutic implications and challenges, Acta Pharmacol. Sin. 34 (2013) 732–740.

[35] H. Acloque, M.S. Adams, K. Fishwick, M. Bronner-Fraser, M.A. Nieto, Epithelial-mesenchymal transitions: the importance of changing cell state in development and disease, J. Clin. Invest. 119 (2009) 1438–1449.

[36] W. Guo, Z. Keckesova, J.L. Donaher, T. Shibue, V. Tischler, F. Reinhardt, S. Itzkovitz, A. Noske, U. Zurrer-Hardi, G. Bell, W.L. Tam, S.A. Mani, A. van Oudenaarden, R.A. Weinberg, Slug and Sox 9 cooperatively determine the mammary stem cell state, Cell 148 (2012) 1015–1028.

[37] C. Scheel, R.A. Weinberg, Phenotypic plasticity and epithelial-mesenchymal transitions in cancer and normal stem cells? Int. J. Canc. 129 (2011) 2310–2314.

[38] L. Li, R. Bhatia, Stem cell quiescence, Clin. Canc. Res. 17 (2011) 4936–4941.

[39] I. Roato, R. Ferracini, Cancer stem cells, bone and tumor microenvironment: key players in bone metastases, Cancers (2018) 10.

[40] A.Z. Ayob, T.S. Ramasamy, Cancer stem cells as key drivers of tumour progression, J. Biomed. Sci. 25 (2018) 20.

[41] Y. Shiozawa, R.S. Taichman, Cancer stem cells and the bone marrow microenvironment, BoneKEy Rep. (2012) 2012.

[42] K. Weidenfeld, D. Barkan, EMT and stemness in tumor dormancy and outgrowth: are they intertwined processes? Front Oncol 8 (2018) 381.

[43] R. Thakur, R. Trivedi, N. Rastogi, M. Singh, D.P. Mishra, Inhibition of STAT3, FAK and Src mediated signaling reduces cancer stem cell load, tumorigenic potential and metastasis in breast cancer, Sci. Rep. 5 (2015) 10194.

[44] L. Li, T. Duan, X. Wang, R.H. Zhang, M. Zhang, S. Wang, F. Wang, Y. Wu, H. Huang, T. Kang, KCTD12 regulates colorectal cancer cell stemness through the ERK pathway, Sci. Rep. 6 (2016) 20460.

[45] L. Bai, G. Shi, L. Zhang, F. Guan, Y. Ma, Q. Li, Y.S. Cong, L. Zhang, Cav-1 deletion impaired hematopoietic stem cell function, Cell Death Dis. 5 (2014) e1140.

[46] F. Sotgia, T.M. Williams, A.W. Cohen, C. Minetti, R.G. Pestell, M.P. Lisanti, Caveolin-1-deficient mice have an increased mammary stem cell population with upregulation of Wnt/beta-catenin signaling, Cell Cycle 4 (2005) 1808–1816.

[47] P.G. Lloyd, C.D. Hardin, Caveolae in cancer: two sides of the same coin? Focus on "Hydrogen peroxide inhibits non-small cell lung cancer cell anoikis through the inhibition of caveolin-1 degradation", Am. J. Physiol. Cell Physiol. 300 (2011) C232–C234.

[48] A.F. Quest, L. Lobos-Gonzalez, S. Nunez, C. Sanhueza, J.G. Fernandez, A. Aguirre, D. Rodriguez, L. Leyton, V. Torres, The caveolin-1 connection to cell death and survival, Curr. Mol. Med. 13 (2013) 266–281.

[49] C.H. Lee, C.C. Yu, B.Y. Wang, W.W. Chang, Tumorsphere as an effective in vitro platform for screening anti-cancer stem cell drugs, Oncotarget 7 (2016) 1215–1226.

[50] I. Rabinovich, A.P.M. Sebastiao, R.S. Lima, C.A. Urban, E.S. Junior, K.F. Anselmi, S. Elifio-Esposito, L. De Noronha, A.N. Moreno-Amaral, Cancer stem cell markers ALDH1 and CD44 + /CD24- phenotype and their prognosis impact in invasive ductal carcinoma, Eur. J. Histochem. 62 (2018).

[51] W. Li, H. Ma, J. Zhang, L. Zhu, C. Wang, Y. Yang, Unraveling the roles of CD44/CD24 and ALDH1 as cancer stem cell markers in tumorigenesis and metastasis, Sci. Rep. 7 (2017) 13856.

[52] S.A. Patel, S.H. Ramkissoon, M. Bryan, L.F. Pliner, G. Dontu, P.S. Patel, S. Amiri, S.R. Pine, P. Rameshwar, Delineation of breast cancer cell hierarchy identifies the subset responsible for dormancy, Sci. Rep. 2 (2012) 906.

[53] E. Farahani, H.K. Patra, J.R. Jangamreddy, I. Rashedi, M. Kawalec, R.K. Rao Pariti, P. Batakis, E. Wiechec, Cell adhesion molecules and their relation to (cancer) cell stemness, Carcinogenesis 35 (2014) 747–759.

[54] S. Chen, M. Lewallen, T. Xie, Adhesion in the stem cell niche: biological roles and regulation, Development 140 (2013) 255–265.

[55] S. Lamouille, J. Xu, R. Derynck, Molecular mechanisms of epithelial-mesenchymal transition, Nat. Rev. Mol. Cell Biol. 15 (2014) 178–196.

[56] R. Ortiz, J. Diaz, N. Diaz, L. Lobos-Gonzalez, A. Cardenas, P. Contreras, M.I. Diaz, E. Otte, J. Cooper-White, V. Torres, L. Leyton, A.F. Quest, Extracellular matrix-specific Caveolin-1 phosphorylation on tyrosine 14 is linked to augmented melanoma metastasis but not tumorigenesis, Oncotarget 7 (2016) 40571–40593.

[57] A. Maiuthed, N. Bhummaphan, S. Luanpitpong, A. Mutirangura, C. Aporntewan, A. Meeprasert, T. Rungrotmongkol, Y. Rojanasakul, P. Chanvorachote, Nitric oxide promotes cancer cell dedifferentiation by disrupting an Oct4:caveolin-1 complex: a new regulatory mechanism for cancer stem cell formation, J. Biol. Chem. 293 (2018) 13534–13552.

[58] F.R. Bakhshi, M. Mao, A.N. Shajahan, T. Piegeler, Z. Chen, O. Chernaya, T. Sharma, W.M. Elliott, R. Szulcek, H.J. Bogaard, S. Comhair, S. Erzurum, G.P. van Nieuw Amerongen, M.G. Bonini, R.D. Minshall, Nitrosation-dependent caveolin 1 phosphorylation, ubiquitination, and degradation and its association with idiopathic pulmonary arterial hypertension, Pulm. Circ. 3 (2013) 816–830.

[59] A.M. Zimnicka, Y.S. Husain, A.N. Shajahan, M. Sverdlov, O. Chaga, Z. Chen, P.T. Toth, J. Klomp, A.V. Karginov, C. Tiruppathi, A.B. Malik, R.D. Minshall, Src-dependent phosphorylation of caveolin-1 Tyr-14 promotes swelling and release of caveolae, Mol. Biol. Cell 27 (2016) 2090–2106.

[60] L. Orlichenko, B. Huang, E. Krueger, M.A. McNiven, Epithelial growth factor-induced phosphorylation of caveolin 1 at tyrosine 14 stimulates caveolae formation in epithelial cells, J. Biol. Chem. 281 (2006) 4570–4579.

[61] M.A. del Pozo, N. Balasubramanian, N.B. Alderson, W.B. Kiosses, A. Grande-Garcia, R.G. Anderson, M.A. Schwartz, Phospho-caveolin-1 mediates integrin-regulated membrane domain internalization, Nat. Cell Biol. 7 (2005) 901–908.